CHEMISTRY
A European Journal

A Journal of
ChemPubSoc Europe

Accepted Article

Title: Impact of a Water-Soluble Gallic Acid-Based Dendrimer on the Color-Stabilizing Mechanisms of Anthocyanins

Authors: Luis Cruz, Nuno Basílio, Johan Mendoza, Nuno Mateus, Victor de Freitas, Maun H. Tawara, Juan Correa, and Eduardo Fernandez-Megia

To be cited as: *Chem. Eur. J.* 10.1002/chem.201901912

Link to VoR: http://dx.doi.org/10.1002/chem.201901912

Supported by
ACES

WILEY-VCH

Impact of a Water-Soluble Gallic Acid-Based Dendrimer on the Color-Stabilizing Mechanisms of Anthocyanins

Luís Cruz,[a,*] Nuno Basílio,[c] Johan Mendoza,[c] Nuno Mateus,[a] Victor de Freitas,[a] Maun H. Tawara,[b] Juan Correa,[b] Eduardo Fernandez-Megia[b]

[a]*REQUIMTE/LAQV, Departamento de Química e Bioquímica, Faculdade de Ciências, Universidade do Porto, Rua do Campo Alegre, s/n, 4169-007 Porto, Portugal.*
[b]*Centro Singular de Investigación en Química Biolóxica e Materiais Moleculares (CIQUS) and Departamento de Química Orgánica, Universidade de Santiago de Compostela, Jenaro de la Fuente s/n, 15782 Santiago de Compostela, Spain.*
[c]*LAQV, REQUIMTE, Departamento de Química, Faculdade de Ciências e Tecnologia, Universidade Nova de Lisboa, 2829-516 Caparica, Portugal.*

*Corresponding author. Tel.: +351 220402558; fax: +351 220402658.
Email address: luis.cruz@fc.up.pt (Luis Cruz)

ABSTRACT

The interaction of two anthocyanins with a water-soluble polyanionic dendrimer was studied through UV-Vis, stopped-flow and NMR spectroscopy. Cy3glc revealed a stronger interaction than mv3glc at pH 1 according to their apparent association constants. A higher color increased was also obtained for cy3glc at pH 3.5 as a result of this stronger interaction. A high-frequency chemical shift of the cy3glc aromatic protons suggest the formation of ionic pairs. The interaction parameters (K~700 M^{-1}, n~295) indicated the binding of approximately two anthocyanin molecules by each sulfate group. The equilibrium and rate constants of cy3glc in the presence of dendrimer showed an increased stability of the flavylium cation and a higher protection of this species from hydration (pK'_a and pK_h increased almost one pH unit). The tuning and color stabilization of anthocyanins using this dendrimer envisage novel applications as colorimetric sensors for food packaging.

Keywords: UV-Vis spectroscopy; NMR; gallic acid-based dendrimer; anthocyanins; association constant

10.1002/chem.201901912

Introduction

Anthocyanins are glycosylated derivatives of 2-phenyl-benzopyrilium cation being responsible for a pallet of beautiful colors found in many fruits and flowers. This wide range of colors is essentially driven by a pH-dependent multistate involving four different chemical reactions and five species (Scheme 1).[1, 2]

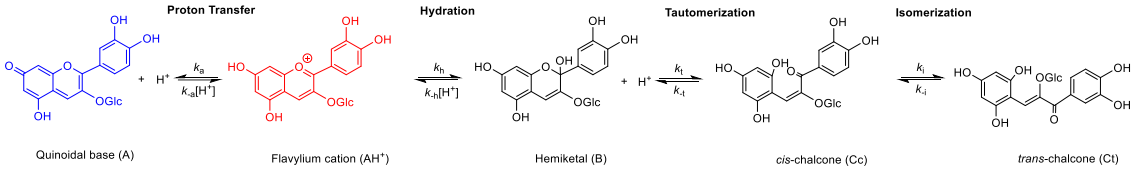

$$K_n = \frac{k_n}{k_{-n}} \quad n = a, h, t, i$$

Scheme 1. Multistate of chemical species of cyanidin-3-glucoside (cy3glc). At very acidic pH the system converges to the flavylium cation.

The reactions shown in Scheme 1 can be described in the following equations (1-4):

Proton transfer $\quad AH^+ + H_2O \overset{K_a}{\rightleftharpoons} A + H_3O^+ \quad (1)$

Hydration $\quad AH^+ + H_2O \overset{K_h}{\rightleftharpoons} B + H_3O^+ \quad (2)$

Tautomerization $\quad B \overset{K_t}{\rightleftharpoons} C_c \quad (3)$

Isomerization $\quad C_c \overset{K_i}{\rightleftharpoons} C_t \quad (4)$

Considering the above chemical equilibria of anthocyanins, a great color fading is expectable at moderated acidic to neutral pH essentially due to the hydration reaction of the flavylium cation to form an uncolored hemiketal species (equation 2). However, in Nature, many plants have found some color-stabilizing mechanisms to maintain their red and blue colors [3-6] at higher pH, such as intermolecular copigmentation,[7] intramolecular copigmentation [8] and self-association [9]. These non-covalent interactions (van der Waals π-π stacking stabilized by intermolecular hydrogen bonds) partially protects the flavylium cation from the hydration reaction. For example, in wine (pH ~ 3.5) anthocyanins are mainly present in their colorless hemiketal form. However, due to the copigmentation phenomena with other flavonoids[10, 11] and to self-association mechanism[3, 12], the stabilization of the flavylium form of anthocyanins occurs[13]. Other strategies for color stabilization of anthocyanins found by plants is to make acylated derivatives which are

usually used as food colorants because of superior stability over non-acylated anthocyanins.[14, 15] Supramolecular host-guest interactions have been widely applied in chemical and biochemical fields. Host−guest systems are formed by molecular recognition of a receptor (host) and a ligand (guest) by means of noncovalent interactions, such as electrostatic, hydrogen-bonds, hydrophobic interactions, chemical coordination, van der Waals forces and π−π stacking. Guests gain benefits from the host−guest system by binding to the host to improve their stability, solubility, bioavailability, etc. Several hosts have been described for inclusion of guest molecules such as crown ethers, porphyrins, cyclodextrins, cucurbiturils, nanoparticles and nanotubes, liposomes and dendrimers[16]. The stabilization of natural anthocyanins and flavylium analogues by developing host-guest systems is poorly reported in literature[17-19]. In the case of cyclodextrins, a destabilization of the red flavylium cation generally occurs because the colorless hemiketal species is preferentially encapsulated by the receptor. To the best of our knowledge, dendrimers have never been used as hosts for color tuning of anthocyanins with pH. A recent study demonstrated the use of silica-PAMAM dendrimer nanoparticles to encapsulate anthocyanins and to further evaluated their antiproliferative activity against neuroblastoma (Neuro 2A).[20] Dendrimers are synthetic tree-like macromolecules composed of repetitive layers of branching units that emerge from a central core. They are synthesized in a controlled iterative fashion through generations with nil dispersity, precise molecular weight, and discrete properties. Their high functional surface, globular architecture in the nanometer scale, and inherent multivalency make them ideal candidates for a wide range of applications, from bio- and nanotechnology to catalysis and materials science[21, 22]. Water-soluble dendrimers are recognized as ideal candidates for bioapplications. Furthermore, polyanionic dendrimers have been showed higher biocompatible profiles compared to polycationic ones.[23-25]

In this work, a water-soluble GATG (gallic acid-triethylene glycol) dendrimer[26]decorated with 162 terminal anionic sulfate groups was used to study its effect on the color-stabilizing mechanisms of two important anthocyanin monoglucosides found in Nature (malvidin-3-glucoside and cyanidin-3-glucoside) at molecular level, as well as their thermodynamic and kinetic properties (Figure 1). Dendrimers field is a hot topic to explore innovative applications for anthocyanins for example to develop novel pH-sensor systems for food intelligent packaging.[27]

10.1002/chem.201901912

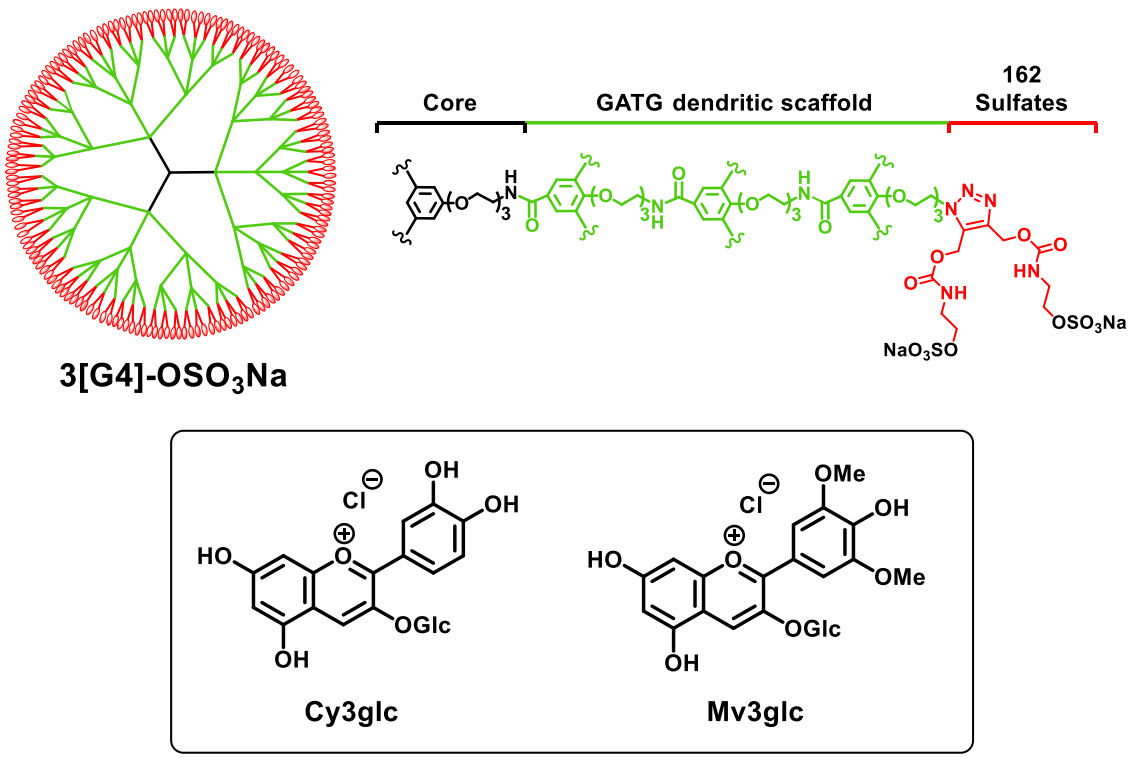

Figure 1. Structures of 3[G4]-OSO_3Na carrying 162 peripheral sodium sulfate groups and anthocyanins (flavylium salts).

Experimental Section

Materials

Theorell and Stenhagen universal buffer [28] was prepared by dissolving 2.25 mL of phosphoric acid (85 % w/w), 3.54 g of boric acid, 7.00 g of monohydrated citric acid and 343 mL of NaOH 1M solution in distilled water until 1 L. The other reagents were obtained from Sigma-Aldrich (Madrid, Spain). 3[G4]-OSO_3Na, a GATG dendrimer of fourth generation with 162 terminal sodium sulfate groups (MW: 61672 $g.mol^{-1}$) was obtained from 3[G3]-N_3 [29, 30] via azide-alkyne cycloaddition. A solution of 3[G3]-N_3 (47 mg, 1.97 µmol) and ammonium 4,11-dioxo-5,10-dioxa-3,12-diazatetradec-7-yne-1,14-diyl bis(sulfate) (145 mg, 0.319 mmol) in tBuOH/H_2O 1:1 (160 µL) was stirred at 120 ºC for 8 h and then was purified by ultrafiltration (4 x 30 mL 0.1 M NaOH and 2 x 30 mL H_2O, Amicon YM3) and lyophilized to afford 3[G4]-OSO_3Na as a white foam (108 mg, 91%): ^1H NMR (500 MHz, D_2O) δ: 7.26-7.12 (m, 78H), 6.26 (br s, 3H), 5.43-5.16 (m, 324H), 4.71-4.58 (m, 162H), 4.29-4.01 (m, 564H), 4.00-3.51 (m, 1038H), 3.48-3.32 (m, 324H). ^{13}C NMR (75 MHz, D_2O) δ: 168.8, 157.5, 157.0, 151.8, 141.9, 139.6, 132.6,

129.3, 106.1, 72.1, 69.9, 69.5, 69.0, 68.8, 68.3, 67.2, 67.1, 57.1, 53.9, 48.6, 40.0. IR (KBr): 3446, 2935, 1718, 1542, 1255 cm^{-1}. Malvidin-3-glucoside (mv3glc) and cyanidin-3-glucoside (cy3glc) were obtained by extraction from a young red wine (*Vitis vinifera* L. cv. Touriga Nacional) and from blackberries (*Rubus fruticosus* L.), respectively. All the purification procedures were followed as described elsewhere.[31, 32] The purity of the pigments was assessed by HPLC-DAD and ^1H NMR.

pH jumps

The equilibrium and rate constants of cy3glc in the presence and absence of 3[G4]-OSO_3Na dendrimer were studied by UV−visible spectroscopy using the pH jump technique from pH = 1 to higher pH values. To a 1 cm path length cell were added 300 μL of 0.1 M NaOH solution, 300 μL of Theorell and Stenhagen universal buffer solution at the desired pH value and 150 μL of a dendrimer stock solution at pH = 1 (0.1 M HCl). At the end, 150 μL of the anthocyanin stock solution at pH 1.0 (0.1 M HCl) was added to the cell giving a final concentration of 19.8 μM of cy3glc and 26 μM of dendrimer. The same experiment was done without the addition of the dendrimer. In this case, the dendrimer solution was changed by 0.1 M HCl solution. The UV-Vis spectra of the different solutions were taken from 300 to 800 nm in a Thermo Scientific Evolution Array UV−visible spectrophotometer and their kinetics were followed until the equilibrium of the system was reached. The pH values of all solutions were measured in a Radiometer Copenhagen PHM240 pH/ion meter. The fitting of experimental data was carried out using nonlinear least-squares method and the Solver function from Microsoft Excel.

Stopped-Flow

Stopped-flow experiment was conducted in an Applied Photophysics SX20 stopped-flow spectrophotometer provided with a PDA.1/UV photodiode array detector with a minimum scan time of 0.65 ms and a wavelength range of 200 nm to 735 nm. The reverse pH jump was carried out by placing an equilibrated solution of the pigment in the presence of dendrimer at pH 5.58 in one syringe and the respective amount of HCl in the second syringe to obtain the desired final pH ~ 1. A small volume of the sample was recovered after the mixture to confirm the pH of the solution.

Copigmentation studies

The solutions were prepared in citrate buffer solution (0.2 M) at pH 3.5, and the ionic strength was set to 0.5 M by addition of sodium chloride. Each pigment:dendrimer solution was obtained by mixing a volume of the pigment stock solution (fixed final concentration of 19.8 μM for cy3glc and 10.3 μM for mv3glc) with an aliquot of a dendrimer stock solution to give increasing concentrations of dendrimer between 5 and 40 μM. Each experiment was performed in triplicate and the solutions were left to equilibrate for 30 min before the measurement. UV-visible spectra were recorded from 360 to 830 nm (1 nm sampling interval) using a 1 cm path length cell on a BIO-TEK Power Wave XS spectrophotometer at a temperature of 25 ºC.

Titration experiments

UV-Vis spectroscopy

The apparent association constants of the anthocyanin−dendrimer complex were estimated by UV−visible spectroscopy in aqueous solutions at pH 1. A solution of anthocyanin (cyglc 19.8 μM; mv3glc 10.3 μM) was prepared in 0.1 M HCl (solution A). Similarly, a solution containing a mixture of anthocyanin (cyglc 19.8 μM; mv3glc 10.3 μM) and dendrimer at the concentration of 24 μM was prepared (solution B). Then, to the solution A was subsequently added a known volume of solution B allowing to achieve increasing concentrations of dendrimer (from 0.59 to 12 μM). UV−visible absorption spectra were taken in a Thermo Scientific Evolution Array UV−visible spectrophotometer from 360 to 830 nm in a 1 cm path length cell. The absorbance values variations (Abs) as a function of dendrimer concentration [L_0] can be expressed by equation (5), previously developed by similar host-guest interactions[33]:

$$Abs = Abs_0 + \Delta Abs \frac{nK[L_0]}{1+nK[L_0]} \quad (5)$$

where n*K* is the apparent binding constant, n is the number of nonspecific binding sites of the dendrimer where anthocyanin can bind, and [L_0] the total concentration of the dendrimer added. The data could be fitted by equation (5) using the nonlinear least-squares method and the Solver function from Microsoft Excel:

NMR

For the NMR studies, a 0.124 mM solution of cy3glc was prepared in D_2O and the pH was adjusted to 1 (pD 1.4) and transferred into 5 mm NMR tubes. Sodium trimethylsilyl-[2,2,3,3-d4]-propionate (TSP, 5 μL, 0.05 mM in D_2O) was used as an internal standard for chemical shift measurements. Successive volumes of a dendrimer stock solution in D_2O (16.2 μM) were added to the NMR tube to obtain different anthocyanin:dendrimer molar ratios during the titration. pH measurements were made in a pH-meter WTW pH 320 fitted with a standard glass Crison® 5209 electrode. The calibration was made with standard aqueous buffers at pH 4.0 and pH 1.0 from Crison®. All ^{1}H NMR spectra were recorded at 298.2K on a Bruker Avance III 400 HD spectrometer, operating at 400.14 MHz, equipped with 5 mm PADUL and pulse gradient units, capable of producing magnetic field pulsed gradients in the z-direction of 50 G/cm. The measurements were done with standard Bruker pulse sequences at 298.2 K. ^{1}H NMR experiments were performed with water suppression using excitation sculpting with gradients, acquisition time 2.56 s, relaxation delay 1s and 64 transients of a spectral width of 6410.26 Hz were collected into 32 K time domain points,

NMR data analysis

For titration experiments, chemical shift variations ($\Delta\delta_{obs}$) of some cy3glc protons as a function of cy3glc/dendrimer molar ratio can be expressed through equation (6)[16]:

$$\Delta\delta_{obs} = \frac{\Delta\delta_{max}}{2}\left\{\left(1 + \frac{1}{K[Guest]} + \frac{n[Dend]}{[Guest]}\right) - \left[\left(1 + \frac{1}{K[Guest]} + \frac{n[Dend]}{[Guest]}\right)^2 - \frac{4n[Dend]}{[Guest]}\right]^{1/2}\right\} \quad (6)$$

$\Delta\delta_{max}$ is the maximum chemical shift variation of the guest molecule in NMR titration experiment *K* is the binding affinity or association constant The number of binding sites (n) was obtained by fitting the titration data with equation (6) using a nonlinear least-squares method within the software program Microsoft Excel.

Results and discussion

UV-Visible spectroscopy.

Preliminary studies to evaluate possible interactions between cy3glc and three types of GATG-based dendrimers, namely cationic amine 3[G4]-NH_2·HCl, anionic sulfated 3[G4]-OSO_3Na and neutral triethylene glycol 3[G4]-OH (each decorate with 162 terminal residues) were performed in aqueous solutions at pH 1 and 3.5. The results showed only

a significant and interesting stabilization and intensification of the cy3glc color obtained in the presence of the anionic dendrimer at both pH values rather than with the other two dendrimers (supporting information). Bearing this, the interaction of mv3glc and cy3glc with the dendrimer 3[G4]-OSO_3Na was studied in detail at pH 1 through UV-Vis spectroscopy by increasing the dendrimer concentration over a solution of anthocyanin at a fixed concentration. Figure 2 illustrates a bathochromic shift with the successive addition of small amounts of dendrimer solution. Upon the binding to the dendrimer, the absorption spectrum of the flavylium cation undergoes a red-shift of ca. 10 nm suggesting the incorporation of the anthocyanin in a microenvironment with lower polarity than water. Similar effects were observed upon binding of flavylium cations to anionic micelles, lignin and cucurbiturils.[33-35] The anionic character of the terminal sulfate groups in 3[G4]-OSO_3Na are expected to stabilize the flavylium cation of the anthocyanin by Coulombic interactions. Furthermore, hydrophobic interactions between the 39 gallic acid and 81 triazol residues of the dendrimer and the aromatic framework of the flavylium cation might help stabilizing the interaction. From the absorbance taken at the maximum wavelength of the free pigments as a function of the concentration of the dendrimer and applying the fitting procedures, it was possible to estimate the apparent binding constants of the complexes as nK = 207183 M^{-1} and nK = 52424 M^{-1} for cy3glc and mv3glc, respectively (Figures 2c and 2d).

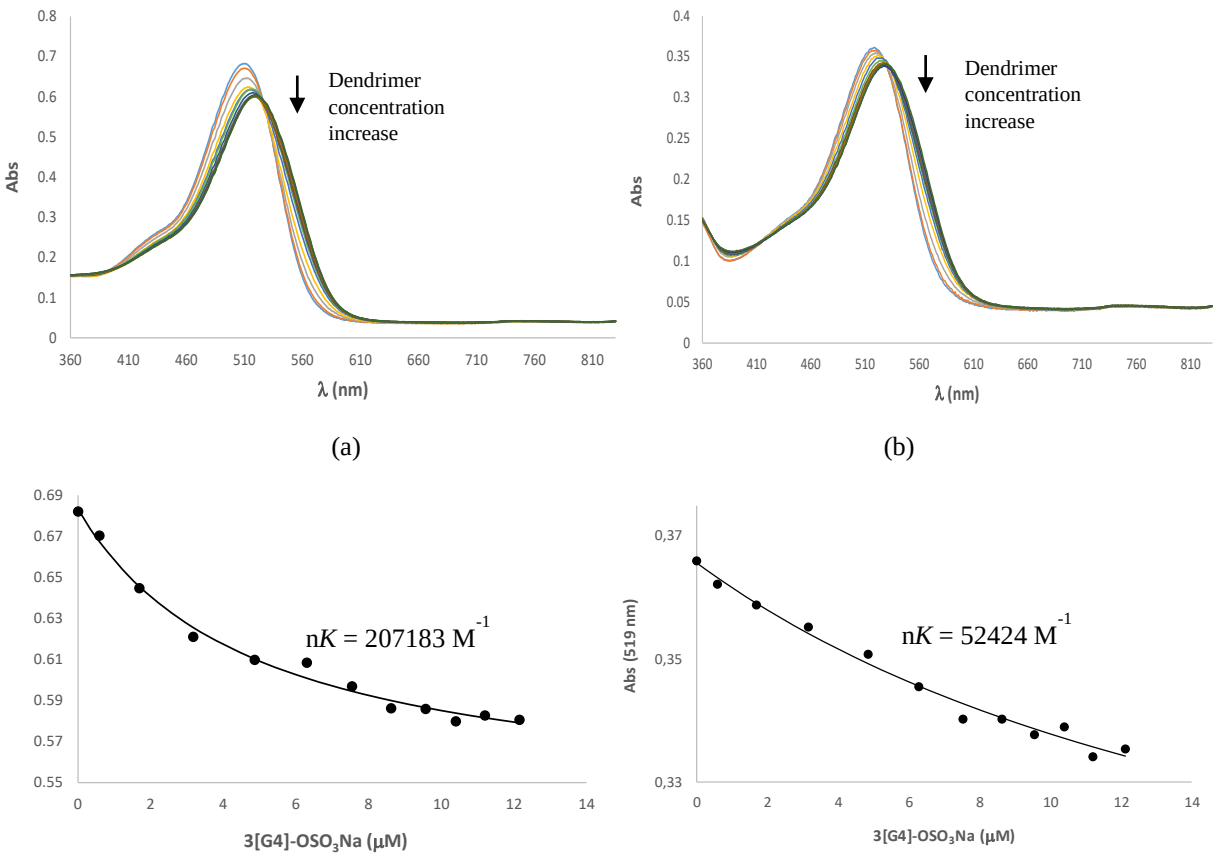

10.1002/chem.201901912

(c) (d)

Figure 2. (a) UV-Visible spectra of cy3glc (19.8 μM) and cy3glc (19.8 μM) with increasing concentrations of 3[G4]-OSO_3Na from 0.59 to 12 μM at pH 1 (0.1 M HCl); (b) the same for mv3glc (at 10.3 μM); (c) fitting of the absorbance as a function of the concentration of 3[G4]-OSO_3Na for cy3glc-dendrimer complex using equation (5) with an estimated error ≈ 10 %; (d) the same for mv3glc-dendrimer complex.

Comparing the two values obtained it can be concluded that cy3glc displays a higher binding affinity to the dendrimer than mv3glc, probably because the presence of the catechol group in cy3glc leads to the establishment of an additional H-bond and/or a stronger bifurcated H-bond. The ability of the dendrimer to interact with anthocyanins was also evaluated at pH 3.5 by means of UV-Vis spectroscopy by adding increasing dendrimer concentrations to a fixed concentration of anthocyanin solution. At this pH, the flavylium and hemiketal forms are the main present species (e.g. pK_h oenin = 2.70 ±0.01)[36, 37], and hence water and the copigment are in competition for the flavylium cation. Usually, in the copigmenation phenomena an increase of the absorbance intensity and a wavelength redshift of the pigment (hyperchromic and bathochromic effects, respectively) occur as a result of the stabilization of the flavylium cation and consequent increase of its mole fraction at the expenses of the neutral species. From Figure 3, it was possible to observe these two effects in the UV-Vis spectra of both anthocyanins with the addition of increasing concentrations of dendrimer.

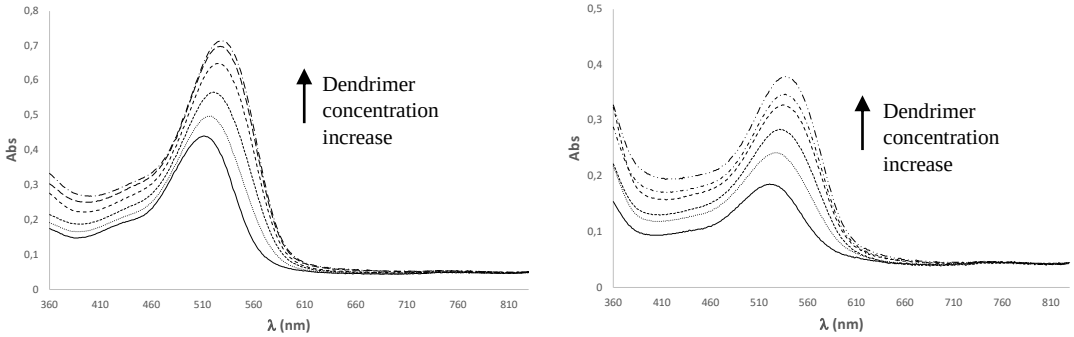

(a) (b)

Figure 3. (a) UV-Visible spectra of free cy3glc (19.8 μM) and cy3glc (19.8 μM) with increasing concentrations of 3[G4]-OSO_3Na (5, 10, 20, 30 and 40 μM) at pH 3.5 (0.2 M citrate buffer); (b) the same for mv3glc (at 10.3 μM).

For the highest concentration of dendrimer (40 μM), an increase of the absorption maxima of the anthocyanins was observed compared to that of the free pigments: 29 % for cy3glc

and 20 % for mv3glc. This is in good agreement with the higher binding affinity of cy3glc towards the dendrimer, contributing to its great color stabilization.

NMR spectroscopy.

The variations in proton chemical shifts of hosts and guests in ^{1}H NMR can be used to investigate host−guest interactions. The decrease of electron density around a nucleus causes an increase of chemical shift (downfield shift or deshielding), while the increase of electron density leads to a decrease of chemical shift (upfield shift or shielding)[38]. When cy3glc was titrated with dendrimer in D_2O at pD 1.4, significant downfield shifts of all aromatic protons of cy3glc were observed (Figure 4). This result suggests the formation of ionic pairs between the polyanionic dendrimer and flavylium cation of cy3glc [39-41]. Analysis of the ^{1}H NMR titration data with the proposed equation (2) could be used to estimate the binding parameters of the complex such as the number of binding sites (n), the maximum chemical shift ($\Delta\delta_{max}$) change and the association constant (*K*) at pH 1.[42-46] To this end, the $\Delta\delta_{obs}$ was plotted against the guest/host molar ratio and the data was fitted using equation (16). From the fitting it was possible to achieve a $\Delta\delta_{max}$=0.0365 and to estimate the number of binding sites (n) of the guest to dendrimer around 295, which means that approximately two molecules of flavylium cation of cy3glc could bind to each terminal sulfate group of the dendrimer bearing the fact that dendrimer has 162 termini sulfate groups. The flavylium cation species should be located at the dendrimer periphery, forming reversibly contact ion pairs with the sulfate group in which the anionic charge should be delocalized by the three oxygen atoms of the sulfate group as it has been suggested in literature for similar host-guest systems (e.g. acetylcholine and benzoate-terminal dendrimers)[41, 42] (Figure 5). From the number of binding sites, the association constant (*K*) could be estimated to be around 700 M^{-1}.

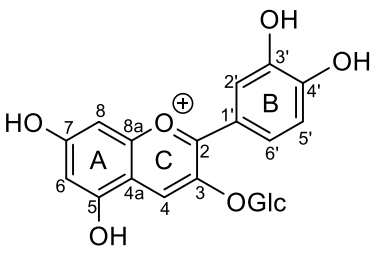

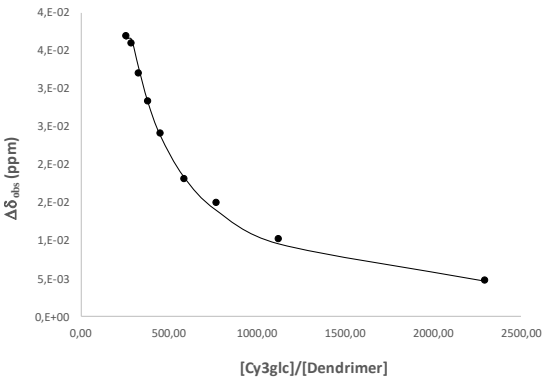

10.1002/chem.201901912

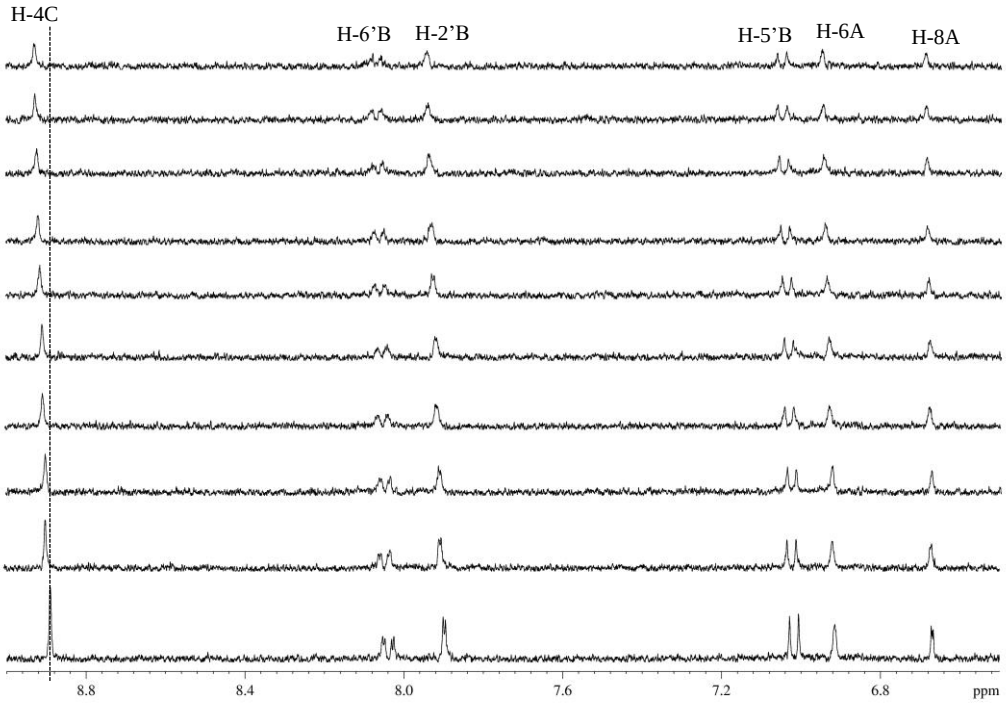

Figure 4. ^{1}H spectra region (9.0–6.5 ppm) of the flavylium cation of cy3glc at initial concentration of 124 μM with increasing dendrimer concentrations from 0 μM (bottom) to 0.47 μM (top) recorded in D_2O at pD 1.4. Representation of the chemical shift variations of H-4C of cy3glc ($\Delta\delta_{obs}$) in function of the guest/host molar ratio (in upper right). Fitting was achieved with equation (6) with an estimated error ≈ 10 %.

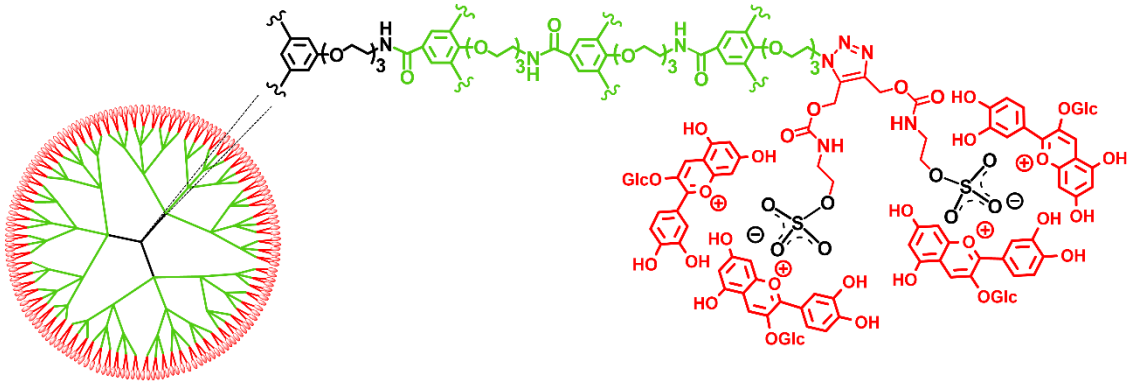

Figure 5. Schematic representation of the interaction between two cy3glc molecules (flavylium cation) and each sulfate-terminated residue of the 3[G4]-OSO_3Na dendrimer.

Equilibrium and rate constants of cy3glc-3[G4]-OSO_3Na complex

The multistate of chemical reactions showed in Scheme 1, can be conveniently investigated through the pH jump methodology.[47] The direct pH jumps are defined as the addition of base to equilibrated solutions of the flavylium cation while reverse pH

10.1002/chem.201901912

jumps result from addition of acid to equilibrated solutions at moderately acidic to neutral pHs and the relaxation process is follow towards the new equilibrium using spectroscopic techniques. Stopped-flow is a crucial tool to follow the kinetic processes that take place in sub-minutes time scale. After a direct pH jump, the flavylium cation (AH^+) transfer a proton to water giving rise to quinoidal base A, which is by far the fastest kinetic step of the multistate, equation (7).

$$k_{1d} = k_a + k_a[H^+] \quad (7)$$

The second kinetic step is triggered by hydration of the electrophilic flavylium cation followed by the ring opening-closure reaction (tautomerization). The former process is much slower and consequently it is the rate determining step, equation (8).

$$k_{2d} = \frac{[H^+]}{[H^+]+K_a} k_h + \frac{1}{1+K_t} k_{-h}[H^+] \quad (8)$$

At this point the system reaches the so-called pseudo-equilibrium ($K^\wedge_a$) because the formation of C_t is much slower, equation (9):

$$\mathbf{AH}^+ + H_2O \overset{K^\wedge_a}{\rightleftharpoons} \mathbf{CB} + H_3O^+ \qquad K^\wedge_a = K_a + K_h + K_hK_t \quad (9)$$

with [CB] = [A] + [B] + [C_c]

After the slowest step of the multistate (isomerization reaction) the system relaxes to the equilibrium according to equation (10)

$$k_{3d} = \frac{K_hK_t}{[H^+]+K^\wedge_a} k_i + k_{-i} \quad (10)$$

The equilibrium of the system is defined by apparent acidic constant (K'_a), equation (11): [2, 48-50]

$$\mathbf{AH}^+ + H_2O \overset{K'_a}{\rightleftharpoons} \mathbf{CB} + H_3O^+ \qquad K'_a = K_a + K_h + K_hK_t + K_hK_tK_i \quad (11)$$

with [CB] = [A] + [B] + [C_c] + [C_t]

10.1002/chem.201901912

From the equations (1-4, 9 and 11) the mole fraction of each species in function of pH can be deduced:

$$[\mathrm{AH^+}] = \frac{[\mathrm{H^+}]}{[\mathrm{H^+}]+K_\mathrm{a}'}; \quad (12)$$

$$[\mathrm{A}] = \frac{K_\mathrm{a}}{[\mathrm{H^+}]+K_\mathrm{a}'}; \quad (13)$$

$$[\mathrm{B}] = \frac{K_\mathrm{h}}{[\mathrm{H^+}]+K_\mathrm{a}'}; \quad (14)$$

$$[\mathrm{C_c}] = \frac{K_\mathrm{h}K_\mathrm{t}}{[\mathrm{H^+}]+K_\mathrm{a}'}; \quad (15)$$

$$[\mathrm{C_t}] = \frac{K_\mathrm{h}K_\mathrm{t}K_\mathrm{i}}{[\mathrm{H^+}]+K_\mathrm{a}'} \quad (16)$$

Direct pH jumps

The chemical equilibria network of cy3glc in the presence of the sulfated dendrimer at fixed concentration was studied by UV-Vis spectroscopy through direct pH jumps (from equilibrated acidic solutions to less acidic pH). After a pH jump, the first kinetic process is due to the proton transfer reaction in the time scale of sub-milliseconds (equation 1) in which no other process occurs and, therefore, the flavylium cation (AH^+) and the quinoidal base (A) are the only species formed. Then, the spectral variations were monitored with time until the system reached the pseudo-equilibrium (AH^+/A, B, and C_c are the species in equilibrium). Fitting the absorbance decay of the pair flavylium cation/quinoidal base as a function of pH allowed the determination of p$K^\wedge_a$ = 3.70. Finally, the system reaches the equilibrium due to the formation of *trans*-chalcone C_t which is the slowest step of the multistate. The UV-Vis spectra of the solutions were recorded again and the fitting of experimental data allowed the determination of pK'_a = 3.66 (Figure 6). The small difference between the p$K^\wedge_a$ and pK'_a accounts for a low mole fraction of Ct in the final equilibrium.

10.1002/chem.201901912

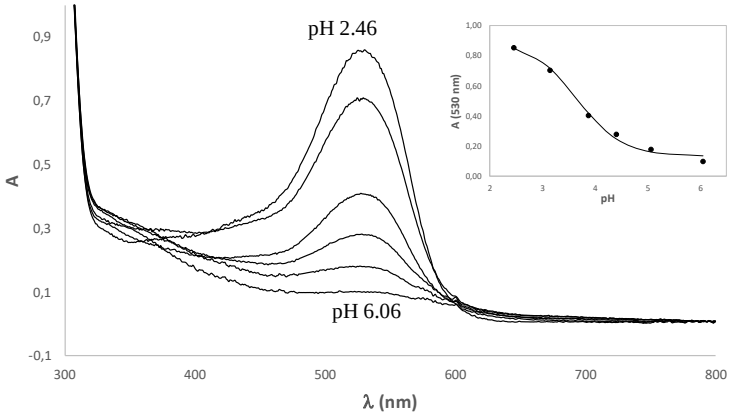

Figure 6. Spectral variations of cy3glc (19.8 μM) in the presence of 3[G4]-OSO_3Na (26 μM) after a direct pH jump at the equilibrium, pK'_a=3.66. Inset: Fitting of the absorbance values at 530 nm as a function of pH.

Normally the pK_a is determined by stopped-flow technique. Alternatively, the pK_a can also be estimated through the pH jump from 1 to 6.06, where the hydration is sufficiently slow, following the absorbance decay of the quinoidal base (Figure 7). From the ratio between A_f and A_i and through equation (13) the pK_a was determined to be 4.71.

The kinetic process of this direct pH jump is showed in inset of Figure 7, which illustrates the second and third kinetic processes described in the introduction (Scheme 1 and eqs. 2-4). The initial absorbance is due to the quinoidal base which formation occurs during the mixing time of the base addition in the direct pH jump. The faster decay is coherent with the second kinetic process (hydration and tautomerization reaction, k_2) where hydration is the rate-determining step. The third kinetic process is due to the slowest step of the equilibrium (isomerization reaction, k_3) and can be observed by the absorbance increase at 350 nm due to the formation of *trans*-chalcone. Fitting the absorbance values as a function of time allowed determining the observed rate constants: $k_2 = 4.3\times10^{-3}$ s^{-1}; $k_3 = 2.5\times10^{-4}$ s^{-1}.

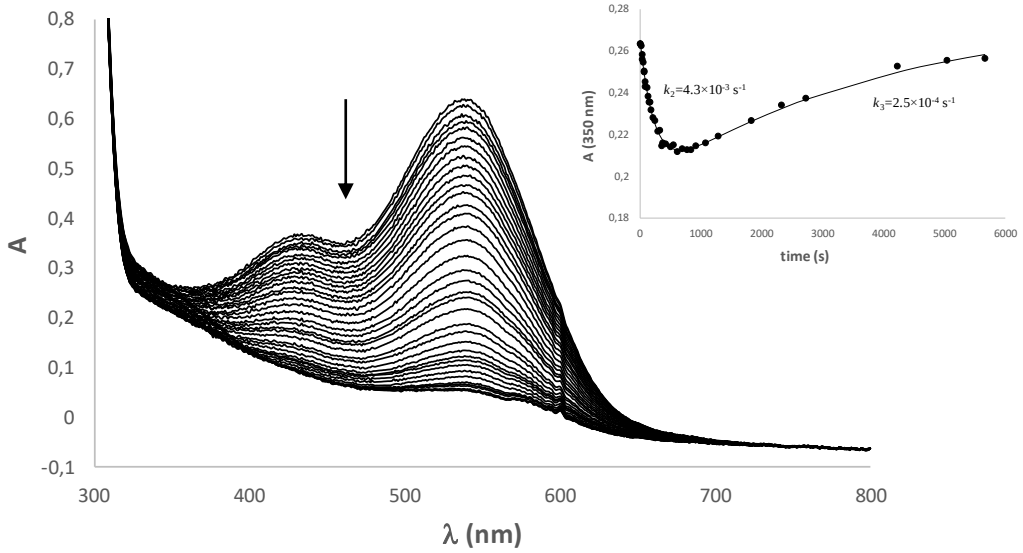

Figure 7. Spectral variations after a direct pH jump from pH=1 to pH=6.06 of cy3glc (19.8 μM) in the presence of 3[G4]-OSO_3Na (26 μM). Inset: variation of absorbance at 350 nm as a function of time showing the second and third kinetic processes.

Then, the second observed rate constant obtained for each pH values was fitted by equation (6) that accounts for the pH-dependence of the rate-limiting hydration process of the flavylium cation to reach the pseudo-equilibrium. By fitting the data presented in Figure 8, it was possible to determine the values of k_h = 0.020 s^{-1} and $k_{-h}/(1+K_t)$ = 110.6 M^{-1} s^{-1}.

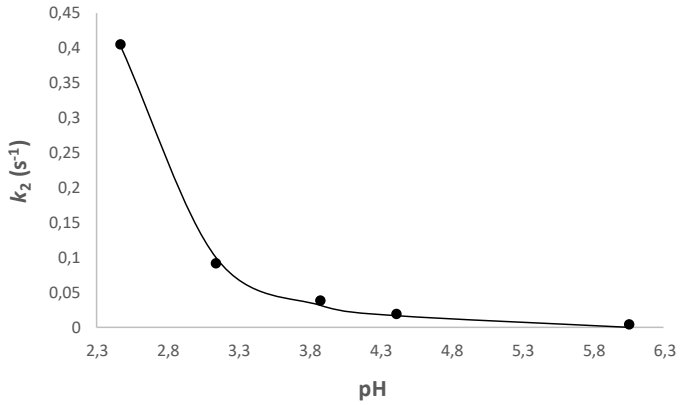

Figure 8. Representation of the observed rate constant of the second kinetic process as a function of pH.

Reverse pH jump

To determine the dehydration rate constant, the tautomerization equilibrium constant K_t and by consequence, the thermodynamic hydration constant (K_h), it was necessary to

10.1002/chem.201901912

carry out a reverse pH jump experiment monitored by stopped-flow from an equilibrated solution at pH=5.58 to pH=0.98 (Figure 9a). Immediately after the addition of acid, all quinoidal base initially at pH=5.58 was rapidly converted into the flavylium cation during the mixing time of the stopped-flow experiment. The faster kinetic step with k_1=10.4 s^{-1} corresponds to the conversion of the hemiketal (B) initially at pH=5.58 into the flavylium cation (AH^+), benefiting from the fact that at sufficiently low pH the hydration is faster than the tautomerization (change of regime).[51] The second kinetic process corresponds to the slower formation of more AH^+ from Cc, through B (k_2=2.98 s^{-1}). From this experiment it was also possible to determine k_{-t} which is equal to the second kinetic rate, k_2. These two kinetic constants were calculated by fitting the absorbance values at 522 nm as a function of time considering a biexponential process (Figure 9b). K_t was determined from the ratio of amplitudes of the second process divided by the first process $\left(K_t = \frac{C_c}{B} = 0.4\right)$ and k_t=1.2 s^{-1} because $K_t = \frac{k_t}{k_{-t}}$. With K_t value in hand, it was possible do determine k_{-h}=154.8 s^{-1}. The hydration equilibrium constant, K_h=1.29×10^{-4} M^{-1} was then obtained from the ratio of both kinetics constants $\left(K_h = \frac{k_h}{k_{-h}}\right)$.

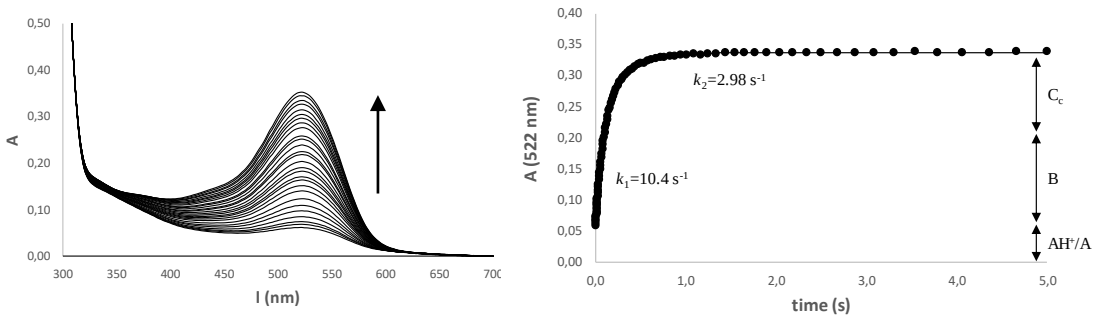

Figure 9. (a) Spectral variations after a reverse pH jump from an equilibrated solution of cy3glc (19.8 μM) in the presence of 3[G4]-OSO_3Na (26 μM) from pH=5.58 to 0.98. (b) Fitting of the kinetic processes.

All the kinetic and thermodynamic parameters determined for cy3glc and cy3glc-dendrimer complex are resumed in Table 2. Comparing the values obtained it can be concluded that the presence of the dendrimer has a great effect on the chemical equilibria network of anthocyanins. The pK'_a is increased in 0.82 pH units, which indicates a higher stabilization of the colored flavylium species. Moreover, the flavylium cation is more stabilized than the hemiketal form in the presence of the dendrimer due essentially to a

10.1002/chem.201901912

faster dehydration and lower hydration rate constants compared to the absence of dendrimer as observed for other analogous systems.[52] Hence, the hydration constant increases in one pH unit in the presence of the dendrimer. Moreover, for the cy3glc-dendrimer complex, K_t is increased which reveals a preferential interaction of the *cis*-chalcone for the host than the hemiketal species. Finally, the mole fraction distribution of cy3glc 19.8 μM in the absence of the dendrimer (Figure 10a) was compared with the one of cy3glc 19.8 μM in the presence of dendrimer 26 μM (Figure 10b). It was possible to observe that in the presence of the dendrimer the mole fraction of the hemiketal form decreased significantly between pH 4-7.5 (75 % to 58 %), accompanied with an increase of the flavylium cation.

Table 2. Equilibrium and rate constants obtained by UV–Vis spectroscopy for cy3glc (19.8 μM) and for cy3glc (19.8 μM) in the presence of 3[G4]-OSO_3Na (26 μM). Estimated error ≈ 10%.

	cy3glc	cy3glc–3[G4]-OSO_3Na
K_a (M^{-1})	1.29×10^{-4}	1.95×10^{-5}
pK_a	3.89	4.71
$K^{\wedge}_a$ (M^{-1})	1.32×10^{-3}	2.00×10^{-4}
p$K^{\wedge}_a$	2.88	3.70
K'_a (M^{-1})	1.41×10^{-3}	2.19×10^{-4}
pK'_a	2.85	3.66
K_t	0.12[a]	0.40
K_h (M^{-1})	1.05×10^{-3}	1.29×10^{-4}
pK_h	2.98	3.89
k_t (s^{-1})	0.07[a]	1.2
k_{-t} (s^{-1})	0.6[a]	2.98
k_h (s^{-1})	0.059	0.020
k_{-h} ($M^{-1}\,s^{-1}$)	55.9	154.8

K_a, acidity constant; $K^{\wedge}_a$, pseudo-equilibrium constant; K'_a, equilibrium constant; K_t, tautomerization constant; K_h, hydration constant; k_t, rate of the tautomerization reaction; k_{-t}, rate of the reserve tautomerization reaction; k_h, rate of the hydration reaction; k_{-h}, rate of the dehydration reaction. [a]obtained from Leydet *et al*., 2012.[53]

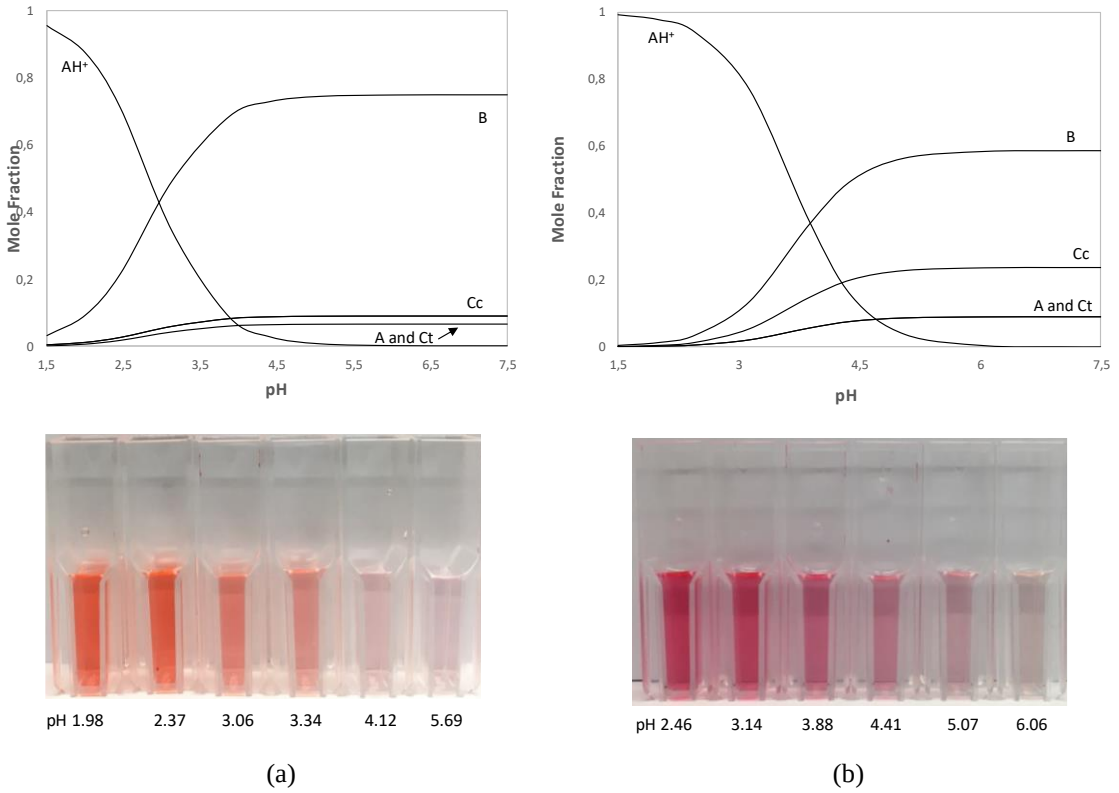

Figure 10. (a) Mole fraction distribution of cy3glc 19.8 μM in function of pH and (b) the same for cy3glc 19.8 μM in the presence of dendrimer 26 μM.

Conclusions

We have determined the influence of a GATG-based polyanionic dendrimer decorated with 162 sulfate groups on the pH-equilibria network of anthocyanins and studied at a molecular level the non-covalent interactions within the host-guest system by UV-Vis, stopped-flow and NMR techniques. Overall, it can be concluded that the dendrimer exerts a great stabilization effect on the thermodynamic and kinetic parameters of cy3glc, increasing its pK_h and pK_a in circa one pH unit. By NMR, it was verified that the red flavylium cation is strongly shielded by the host due to the formation of ionic pairs and the number of binding sites and association constant were determined. The set of results obtained for the color stabilization of anthocyanins and respective tuning in function of pH using this dendrimer open novel applications to be explored such as anthocyanin-based sensors for biomedical devices and smart packaging solutions.

Acknowledgments

The authors thank Dr. Mariana Andrade for the NMR analysis. This research was supported by a research project grant (PTDC/OCE-ETA/31250/2017) with financial support from FCT/MCTES through national funds and co-financed by FEDER, under the

Partnership Agreement PT2020 (UID/QUI/50006/2019 - POCI/01/0145/FEDER/007265). Financial support was also obtained from the Spanish Ministry of Science, Innovation and Universities (CTQ2015-69021-R and RTI2018-102212-B-I00), the Xunta de Galicia (GRC2014/040, ED431C 2018/30, and Centro Singular de Investigación de Galicia Accreditation 2016-2019, ED431G/09) and the European Union (European Regional Development Fund-ERDF). Luís Cruz gratefully acknowledges the research FCT contract.

[1] R. Brouillard, G. A. Iacobucci and J. G. Sweeny, *J. Am. Chem. Soc.* **1982**, *104*, 7585-7590.
[2] F. Pina, M. J. Melo, C. A. T. Laia, A. J. Parola and J. C. Lima, *Chem. Soc. Rev.* **2012**, *41*, 869-908.
[3] A. Fernandes, N. F. Bras, N. Mateus and V. de Freitas, *New J. Chem.* **2015**, *39*, 2602-2611.
[4] F. Di Meo, J. C. S. Garcia, O. Dangles and P. Trouillas, *J. Chem. Theory Comput.* **2012**, *8*, 2034-2043.
[5] M. T. Escribano-Bailon and C. Santos-Buelga, *Curr. Org. Chem.* **2012**, *16*, 715-723.
[6] F. He, N. N. Liang, L. Mu, Q. H. Pan, J. Wang, M. J. Reeves and C. Q. Duan, *Molecules* **2012**, *17*, 1571-1601.
[7] J. Muller-Maatsch, L. Bechtold, R. M. Schweiggert and R. Carle, *Food Chem.* **2016**, *213*, 625-634.
[8] T. Iwashina, *Nat. Prod. Commun.* **2015**, *10*, 529-544.
[9] B. J. Qian, J. H. Liu, S. J. Zhao, J. X. Cai and P. Jing, *Food Chem.* **2017**, *228*, 526-532.
[10] L. Cruz, N. F. Brás, N. Teixeira, N. Mateus, M. J. Ramos, O. Dangles and V. De Freitas, *J. Agric. Food. Chem.* **2010**, *58*, 3159-3166.
[11] N. Teixeira, L. Cruz, N. F. Brás, N. Mateus, M. J. Ramos and V. de Freitas, *J. Agric. Food. Chem.* **2013**, *61*, 6942-6948.
[12] C. Houbiers, J. C. Lima, A. L. Macanita and H. Santos, *J. Phys. Chem. B* **1998**, *102*, 3578-3585.
[13] P. Trouillas, J. C. Sancho-García, V. De Freitas, J. Gierschner, M. Otyepka and O. Dangles, *Chem. Rev.* **2016**, *116*, 4937-4982.
[14] L. Cruz, V. C. Fernandes, P. Araújo, N. Mateus and V. de Freitas, *Food Chem.* **2015**, *174*, 480-486.
[15] L. Cruz, I. Fernandes, M. Guimaraes, V. de Freitas and N. Mateus, *Food Funct.* **2016**, *7*, 2754-2762.
[16] J. Hu, T. Xu and Y. Cheng, *Chem. Rev.* **2012**, *112*, 3856-3891.
[17] J. Mendoza, N. Basílio, O. Dangles, N. Mora, S. Al Bittar and F. Pina, *Dyes Pigm.* **2017**, *143*, 479-487.
[18] A. Fernandes, G. Ivanova, N. F. Bras, N. Mateus, M. J. Ramos, M. Rangel and V. de Freitas, *Carbohydr. Polym.* **2014**, *102*, 269-277.
[19] R. Gomes, R. Q. Albuquerque, F. Pina, A. J. Parola and L. De Cola, *Photochem. Photobiol. Sci.* **2010**, *9*, 991-995.
[20] O. Yesil-Celiktas, C. Pala, E. O. Cetin-Uyanikgil and C. Sevimli-Gur, *Anal. Biochem.* **2017**, *519*, 1-7.
[21] D. Astruc, E. Boisselier and C. Ornelas, *Chem. Rev.* **2010**, *110*, 1857-1959.

[22] A.-M. Caminade, C.-O. Turrin, R. Laurent, A. Ouali and B. Delavaux-Nicot, *Dendrimers: towards catalytic, material and biomedical uses*, John Wiley & Sons, Ltd: Chichester, UK, **2011**, p.
[23] R. Jevprasesphant, J. Penny, R. Jalal, D. Attwood, N. B. McKeown and A. D'Emanuele, *Int. J. Pharm.* **2003**, *252*, 263-266.
[24] N. Malik, R. Wiwattanapatapee, R. Klopsch, K. Lorenz, H. Frey, J. W. Weener, E. W. Meijer, W. Paulus and R. Duncan, *J. Controlled Release* **2000**, *65*, 133-148.
[25] A. Sousa-Herves, D. Gröger, M. Calderón, E. Fernandez-Megia and R. Haag in *Anionic Dendritic Polymers for Biomedical Applications*, The Royal Society of Chemistry, **2013**, pp. 56-72.
[26] A. Sousa-Herves, R. Novoa-Carballal, R. Riguera and E. Fernandez-Megia, *The AAPS Journal* **2014**, *16*, 948-961.
[27] V. Shukla, G. Kandeepan, M. R. Vishnuraj and A. Soni, *Agric. Res.* **2016**, *5*, 205-209.
[28] W. F. Küster and A. Thiel, *Tabelle per le analisi chimiche e chimico-fisiche. 12 ed.; Hoepli: Milano*, **1982**, p.
[29] S. P. Amaral, M. H. Tawara, M. Fernandez-Villamarin, E. Borrajo, J. Martínez-Costas, A. Vidal, R. Riguera and E. Fernandez-Megia, *Angew. Chem. Int. Ed.* **2018**, *57*, 5273-5277.
[30] E. Fernandez-Megia, J. Correa, I. Rodríguez-Meizoso and R. Riguera, *Macromolecules* **2006**, *39*, 2113-2120.
[31] J. Pissarra, N. Mateus, J. C. Rivas-Gonzalo, C. Santos-Buelga and V. De Freitas, *J. Food Sci.* **2003**, *68*, 476-481.
[32] M. Guimarães, N. Mateus, V. de Freitas and L. Cruz, *J. Agric. Food. Chem.* **2018**, *66*, 10003-10010.
[33] P. Araújo, N. Basílio, A. Fernandes, N. Mateus, V. de Freitas, F. Pina and J. Oliveira, *J. Agric. Food. Chem.* **2018**, *66*, 6382-6387.
[34] N. Basílio and F. Pina, *Chemphyschem* **2014**, *15*, 2295-2302.
[35] J. C. Lima, C. Vautier-Giongo, A. Lopes, E. Melo, F. H. Quina and A. L. Maçanita, *J. Phys. Chem. A* **2002**, *106*, 5851-5859.
[36] O. Dangles and H. Elhajji, *Helv. Chim. Acta* **1994**, *77*, 1595-1610.
[37] C. Malien-Aubert, O. Dangles and M. J. Amiot, *J. Agric. Food. Chem.* **2002**, *50*, 3299-3305.
[38] C. Slichter, P., *Principles of Magnetic Resonance; Springer*, NewYork, **2010**, p.
[39] J. Hu, Y. Cheng, Y. Ma, Q. Wu and T. Xu, *J. Phys. Chem. B* **2009**, *113*, 64-74.
[40] J. Hu, Y. Cheng, Q. Wu, L. Zhao and T. Xu, *J. Phys. Chem. B* **2009**, *113*, 10650-10659.
[41] C. Ornelas, E. Boisselier, V. Martinez, I. Pianet, J. Ruiz Aranzaes and D. Astruc, *Chem. Commun.* **2007**, 5093-5095.
[42] E. Boisselier, C. Ornelas, I. Pianet, J. R. Aranzaes and D. Astruc, *Chem. Eur. J.* **2008**, *14*, 5577-5587.
[43] M. A. C. Broeren, B. F. M. de Waal, M. H. P. van Genderen, H. M. H. F. Sanders, G. Fytas and E. W. Meijer, *J. Am. Chem. Soc.* **2005**, *127*, 10334-10343.
[44] X.-D. Xu, H.-B. Yang, Y.-R. Zheng, K. Ghosh, M. M. Lyndon, D. C. Muddiman and P. J. Stang, *J. Org. Chem.* **2010**, *75*, 7373-7380.
[45] A. J. Charlton, N. J. Baxter, M. L. Khan, A. J. G. Moir, E. Haslam, A. P. Davies and M. P. Williamson, *J. Agric. Food. Chem.* **2002**, *50*, 1593-1601.
[46] C. Simon, K. Barathieu, M. Laguerre, J.-M. Schmitter, E. Fouquet, I. Pianet and E. J. Dufourc, *Biochemistry* **2003**, *42*, 10385-10395.
[47] F. Pina, *J. Agric. Food. Chem.* **2014**, *62*, 6885-6897.
[48] R. Brouillard and B. Delaporte, *J. Am. Chem. Soc.* **1977**, *99*, 8461-8468.
[49] R. Brouillard, B. Delaporte and J. E. Dubois, *J. Am. Chem. Soc.* **1978**, *100*, 6202-6205.
[50] R. Brouillard and J. Lang, *Can. J. Chem.* **1990**, *68*, 755-761.
[51] F. Pina, *Dyes Pigm.* **2014**, *102*, 308-314.
[52] J. Mendoza, N. Basílio, F. Pina, T. Kondo and K. Yoshida, *J. Phys. Chem. B* **2018**, *122*, 4982-4992.

10.1002/chem.201901912

609 [53] Y. Leydet, R. Gavara, V. Petrov, A. M. Diniz, A. Jorge Parola, J. C. Lima and F. Pina,
610 *Phytochemistry* **2012**, *83*, 125-135.

611

10.1002/chem.201901912

612 **Graphical Abstract**

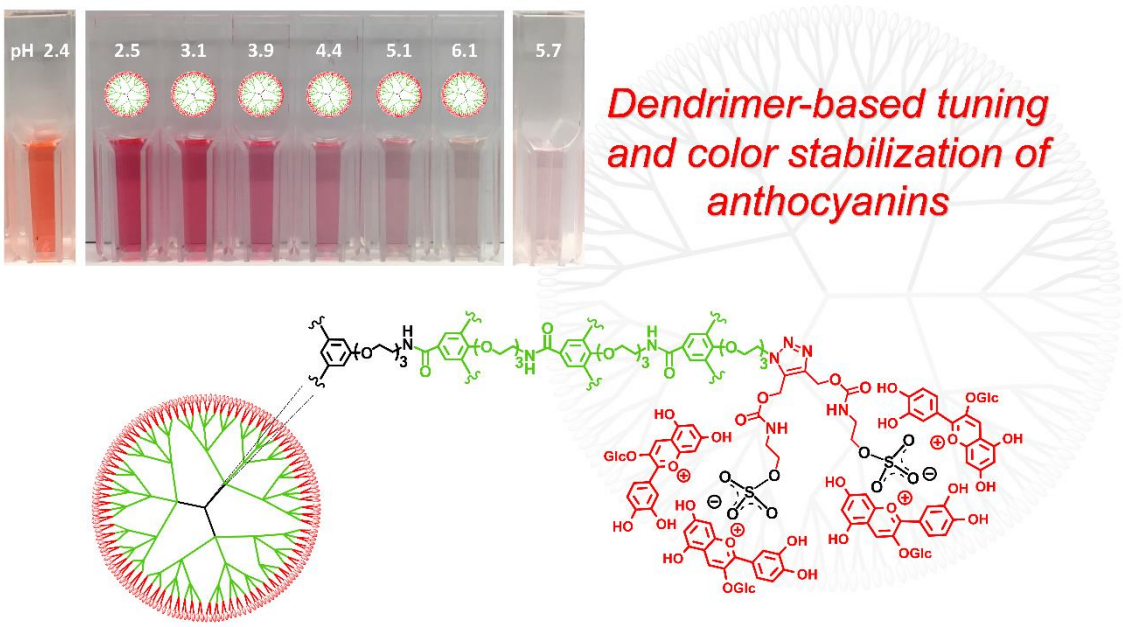

613